

## ANESTHESIOLOGY

# Early Physiologic Effects of Prone Positioning in COVID-19 Acute Respiratory Distress Syndrome

Francesco Zarantonello, M.D., Nicolò Sella, M.D., Tommaso Pettenuzzo, M.D., Giulio Andreatta, M.D., Alvisè Calore, M.D., Denise Dotto, M.D., Alessandro De Cassai, M.D., Fiorella Calabrese, M.D., Annalisa Boscolo, M.D., Paolo Navalesi, M.D.

*Anesthesiology* 2022; 137:327–39

## EDITOR'S PERSPECTIVE

### What We Already Know about This Topic

- The use of prone positioning to treat COVID-19 critically ill mechanically ventilated intubated patients with acute respiratory distress syndrome is now universally accepted. In non-COVID-19 acute respiratory distress syndrome, available evidence suggests it enhances homogeneous distribution of ventilation between dorsal and ventral regions of the lung without significant changes in perfusion.
- Its physiologic effects in COVID-19 have not been systematically investigated.

### What This Article Tells Us That Is New

- Using electrical impedance tomography, the authors assessed the percent variation of ventilation-perfusion matching before and after 90 min of the first cycle of prone positioning in 30 intubated, sedated, and paralyzed adult COVID-19 acute respiratory distress syndrome patients along with additional secondary pulmonary physiologic endpoints.
- Overall, prone positioning improved ventilation-perfusion matching significantly with a median difference of 8% with no change in dorsal perfusion. Lung overdistention was also significantly reduced.
- $P_{aO_2}/F_{iO_2}$  fraction of inspired oxygen improved overall, although 30% of the cohort were classified as nonresponders (less than 20% increase from baseline).

## ABSTRACT

**Background:** The mechanisms underlying oxygenation improvement after prone positioning in COVID-19 acute respiratory distress syndrome have not been fully elucidated yet. The authors hypothesized that the oxygenation increase with prone positioning is secondary to the improvement of ventilation-perfusion matching.

**Methods:** In a series of consecutive intubated COVID-19 acute respiratory distress syndrome patients receiving volume-controlled ventilation, the authors prospectively assessed the percent variation of ventilation-perfusion matching by electrical impedance tomography before and 90 min after the first cycle of prone positioning (primary endpoint). The authors also assessed changes in the distribution and homogeneity of lung ventilation and perfusion, lung overdistention and collapse, respiratory system compliance, driving pressure, optimal positive end-expiratory pressure, as assessed by electrical impedance tomography, and the ratio of partial pressure to fraction of inspired oxygen ( $P_{aO_2}/F_{iO_2}$ ; secondary endpoints). Data are reported as medians [25th to 75th] or percentages.

**Results:** The authors enrolled 30 consecutive patients, all analyzed without missing data. Compared to the supine position, prone positioning overall improved ventilation-perfusion matching from 58% [43 to 69%] to 68% [56 to 75%] ( $P = 0.042$ ), with a median difference of 8.0% (95% CI, 0.1 to 16.0%). Dorsal ventilation increased from 39% [31 to 43%] to 52% [44 to 62%] ( $P < 0.001$ ), while dorsal perfusion did not significantly vary. Prone positioning also reduced lung overdistention from 9% [4 to 11%] to 4% [2 to 6%] ( $P = 0.025$ ), while it did not significantly affect ventilation and perfusion homogeneity, lung collapse, static respiratory system compliance, driving pressure, and optimal positive end-expiratory pressure.  $P_{aO_2}/F_{iO_2}$  overall improved from 141 [104 to 182] mmHg to 235 [164 to 267] mmHg ( $P = 0.019$ ). However, 9 (30%) patients were nonresponders, experiencing an increase in  $P_{aO_2}/F_{iO_2}$  less than 20% with respect to baseline.

**Conclusions:** In COVID-19 acute respiratory distress syndrome patients, prone positioning overall produced an early increase in ventilation-perfusion matching and dorsal ventilation. These effects were, however, heterogeneous among patients.

(ANESTHESIOLOGY 2022; 137:327–39)

Patients with novel COVID-19 associated acute respiratory distress syndrome (ARDS), despite sharing some features with non-COVID-19 ARDS,<sup>1–4</sup> may present clinical characteristics not completely explained by the typical ARDS pathophysiologic mechanisms.<sup>5,6</sup> In COVID-19 ARDS, alveolar injury is associated with severe pulmonary vascular disruption and small- and mid-sized pulmonary

This article is featured in "This Month in Anesthesiology," page A1. Supplemental Digital Content is available for this article. Direct URL citations appear in the printed text and are available in both the HTML and PDF versions of this article. Links to the digital files are provided in the HTML text of this article on the Journal's Web site ([www.anesthesiology.org](http://www.anesthesiology.org)). This article has an audio podcast. This article has a visual abstract available in the online version. F.Z. and N.S. contributed equally to this article.

Submitted for publication December 11, 2021. Accepted for publication June 6, 2022. Published online first on June 16, 2022.

Francesco Zarantonello, M.D.: Institute of Anesthesia and Intensive Care, Padua University Hospital, Padua, Italy.

Nicolò Sella, M.D.: Institute of Anesthesia and Intensive Care, Padua University Hospital, Padua, Italy; Department of Medicine, University of Padua, Padua, Italy.

Tommaso Pettenuzzo, M.D.: Institute of Anesthesia and Intensive Care, Padua University Hospital, Padua, Italy.

Giulio Andreatta, M.D.: Department of Medicine, University of Padua, Padua, Italy.

Copyright © 2022, the American Society of Anesthesiologists. All Rights Reserved. Anesthesiology 2022; 137:327–39. DOI: 10.1097/ALN.0000000000004296

vessels thrombosis,<sup>7,8</sup> mainly ascribable to the COVID-19 related hypercoagulable state.<sup>9</sup>

Radiologic studies assessing lung ventilation and perfusion by subtraction computed tomography angiography showed a high prevalence of perfusion abnormalities, with hypoperfusion predominantly sited in areas of noninjured lungs, and hyperperfusion in the areas of ground-glass opacities, attributed to local inflammation.<sup>10,11</sup> Using electrical impedance tomography, in a small series of COVID-19 patients with ARDS, Mauri *et al.* reported a high rate of mismatched lung units, the extent of dead space exceeding that of shunt.<sup>12</sup> The same group had also found, in non-COVID-19 ARDS patients, the greater mismatch to be correlated with higher mortality.<sup>13</sup>

Prone positioning has been extensively used in COVID-19 ARDS. In a series of 1,057 COVID-19 intubated and mechanically ventilated patients, Langer *et al.* report that 648 patients (61%) received at least one cycle of prone positioning, which was effective in improving oxygenation in the majority of patients for whom data were available, but the underlying mechanisms remain unclear.<sup>14</sup> While in non-COVID-19 ARDS the prone position causes, in general, a more homogenous distribution of ventilation between the dorsal and ventral regions of the lung without significant changes in lung perfusion,<sup>15,16</sup> no definitive data are currently available for COVID-19 ARDS patients.

We previously described the case of one COVID-19 ARDS patient who showed, after only 60 min of prone positioning, improvement of the arterial partial pressure of oxygen to fraction of inspired oxygen ratio ( $\text{PaO}_2/\text{FiO}_2$ ) associated with enhanced ventilation-perfusion matching.<sup>17</sup> Therefore, we hypothesized that in COVID-19 ARDS, arterial oxygenation increases with prone positioning consequent to an improvement of ventilation-perfusion matching, as suggested by a preliminary anecdotal observation.<sup>17</sup> To confirm this hypothesis, we designed this prospective observational study to evaluate the early response to the first cycle of prone positioning in intubated and mechanically ventilated COVID-19 ARDS patients.

## Materials and Methods

### Patients

The study, conducted in the intensive care unit (ICU) of the University Hospital of Padua (Padua, Italy), followed

Alvise Calore, M.D.: Department of Medicine, University of Padua, Padua, Italy.

Denise Dotto, M.D.: Department of Medicine, University of Padua, Padua, Italy.

Alessandro De Cassai, M.D.: Institute of Anesthesia and Intensive Care, Padua University Hospital, Padua, Italy.

Fiorella Calabrese, M.D.: Department of Cardiac, Thoracic, Vascular Sciences and Public Health, University of Padua, Padua, Italy.

Annalisa Boscolo, M.D.: Institute of Anesthesia and Intensive Care, Padua University Hospital, Padua, Italy.

Paolo Navalesi, M.D.: Institute of Anesthesia and Intensive Care, Padua University Hospital, Padua, Italy; Department of Medicine, University of Padua, Padua, Italy.

the “Strengthening the Reporting of Observational Studies in Epidemiology” statement guidelines for observational cohort studies<sup>18</sup> (Supplemental Digital Content, <http://links.lww.com/ALN/C872>). The study, approved by the local Institutional Ethical Committee (reference No. 4853AO20), was conducted in accordance with the principles of the Helsinki Declaration. Written informed consent was obtained according to the national regulation.

We included all consecutive intubated, sedated, and paralyzed adult patients undergoing controlled mechanical ventilation because of ARDS<sup>19</sup> secondary to confirmed ARDS COVID-2 infection,<sup>20</sup> who were admitted between December 1, 2020, and April 1, 2021, and received at least one cycle of prone positioning<sup>15</sup> according to regional guidelines.<sup>21</sup> All patients received low-dose steroids<sup>22</sup> and intermediate doses of low-molecular-weight heparin.<sup>23</sup> All patients were studied in the course of the first cycle of prone positioning. Exclusion criteria were age less than 18 yr, and contraindications to prone positioning<sup>15</sup> and/or to electrical impedance tomography assessment.<sup>24</sup> Patients were considered prone-responders if they showed an increase in  $\text{PaO}_2/\text{FiO}_2$  greater than 20% after 1 h of prone position.<sup>25</sup>

### Endpoints

We assessed the effects determined by 90 min of prone position. Our primary endpoint was assessing the percent variation of ventilation-perfusion matching consequent to prone positioning, as evaluated by electrical impedance tomography. Secondary endpoints were the changes in the distribution and homogeneity of lung ventilation and perfusion, lung overdistention and collapse, respiratory system compliance, driving pressure, optimal positive end-expiratory pressure (PEEP), as assessed by electrical impedance tomography, and  $\text{PaO}_2/\text{FiO}_2$ .

### Protocol and Measurements

The study protocol and variables are depicted in figure 1. No other interventions, such as pharmacologic interventions, bronchoscopic toilette, or physiotherapy, were allowed during the study period. Mechanical ventilation settings,<sup>21</sup> criteria for starting prone positioning,<sup>21</sup> electrical impedance tomography ventilation<sup>12</sup> and perfusion<sup>17</sup> measurements, and electrical impedance tomography PEEP titration technique<sup>24</sup> were all standardized. All patients were mechanically ventilated in volume-controlled mode, with tidal volume 6 ml/kg or less of ideal body weight, at constant inspiratory flow rate set to 60 l/min, and driving pressure maintained at 14 cm  $\text{H}_2\text{O}$  or lower.<sup>21,26</sup> All patients were sedated and under neuromuscular blockade to ensure no spontaneous breathing effort. PEEP was titrated by electrical impedance tomography during a 2-cm  $\text{H}_2\text{O}$ -step decremental PEEP trial from 28 cm  $\text{H}_2\text{O}$  to 8 cm  $\text{H}_2\text{O}$  after a 30 cm  $\text{H}_2\text{O}$  continuous positive airway pressure lung recruitment maneuver lasting 30s, as previously described.<sup>24,27</sup> Briefly, PEEP was set identifying the intersection between the curves representing the cumulative percentage

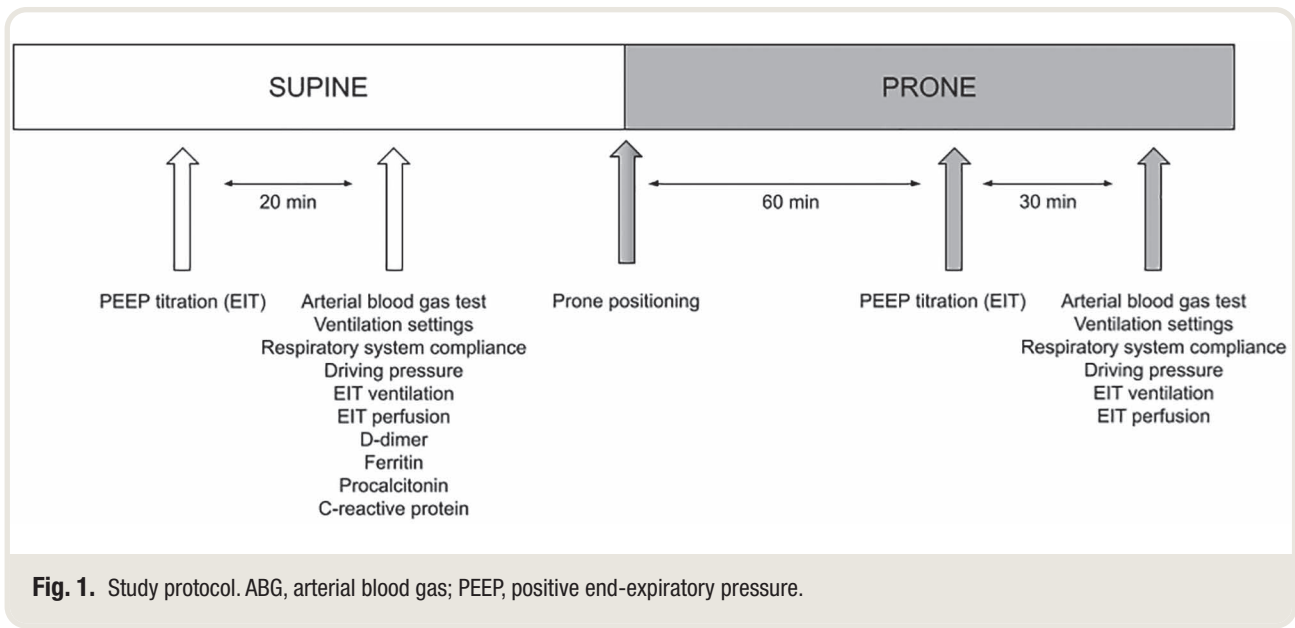


**Fig. 1.** Study protocol. ABG, arterial blood gas; PEEP, positive end-expiratory pressure.

of lung compliance loss due to either collapse or overdistension.<sup>24,27</sup>  $FIO_2$  was set to maintain an arterial oxyhemoglobin saturation measured by pulse oximetry between 88% and 95%.<sup>28</sup> Plateau pressure and total PEEP were measured at points of zero flow during end-inspiratory and end-expiratory pauses, respectively.<sup>26</sup> Driving pressure was calculated as the difference between plateau pressure and total PEEP, while respiratory system quasi-static compliance was calculated as the ratio between tidal volume and driving pressure.<sup>29</sup>

Electrical impedance tomography measurements were obtained through Pulmovista 500 (Draeger, Germany), applying a 16-electrode belt around the patient's thorax in the transversal plane corresponding to the fifth intercostal space. The position of the electrical impedance tomography belt was marked with a dermatographic pen to avoid belt displacement after turning patients prone.<sup>24</sup> For lung perfusion assessment, the indicator technique was used, as previously described in two case reports.<sup>17,30</sup> This technique has already been validated against positron emission tomography in an animal study.<sup>31</sup> Electrical impedance tomography images were continuously recorded at a sampling frequency of 50 Hz. After prone positioning, all measurements were repeated, as depicted in figure 1.

### Electric Impedance Tomography Data Analysis

Both lung ventilation and perfusion-related impedance changes were analyzed through electrical impedance tomography pixel by pixel. In particular, the pixel tidal ventilation was calculated as the difference between end-inspiratory and end-expiratory impedance, and then lung pixels were classified as nonventilated if their tidal variation was 10% or less of the maximal pixel impedance variation.<sup>12</sup>

For PEEP titration, we estimated the variations of regional lung compliance during a decremental PEEP trial

performed after maximal lung recruitment,<sup>24</sup> identifying the loss of compliance at the higher and lower PEEP as the consequence of alveolar overdistension and collapse, respectively. The PEEP value identified by the intersection between the electrical impedance tomography curves representing the cumulative percentage of compliance loss due to overdistension and collapse is defined as optimal PEEP, which assures the best compromise between the two conditions.<sup>24,27</sup>

The per-pixel perfusion was calculated after excluding pixels belonging to the cardiac area using a spatio-temporal approach that removed from the analysis the impedance signals due to the transit of the bolus inside the heart chambers. Pixels with an impedance drop signal 10% or less of the maximal pixel impedance variation were classified as nonperfused.<sup>12</sup>

The lung area was divided into the following zones, as previously described<sup>13</sup>:

- (1) perfused area, defined by all perfused pixels;
- (2) ventilated area, defined by all ventilated pixels;
- (3) percent matched area, defined by all pixels that were both ventilated and perfused divided by the sum of ventilated and perfused pixels;
- (4) percent dead space area, defined by all pixels that were ventilated, but not perfused, divided by the sum of ventilated and perfused pixels;
- (5) percent shunt area, defined by all pixels that were perfused, but not ventilated, divided by the sum of ventilated and perfused pixels;
- (6) percent total unmatched area (total mismatch), *i.e.*, the sum of shunt and dead space area;
- (7) dead space to shunt ratio, *i.e.*, the ratio between dead space area and shunt area.<sup>13</sup>

The thorax was divided into two symmetrical zones, separated by a horizontal line that equally divides it into

ventral and dorsal areas. The following parameters were also calculated:

- dorsal ventilation, representing the percentage of total ventilated lung area that is located in the dorsal half of the thorax;
- dorsal perfusion, representing the percentage of total perfused lung area that is located in the dorsal half of the thorax;
- ventilation and perfusion homogeneity indices. The inhomogeneity index is a value that has been previously described and summarizes the inhomogeneity of lung ventilation and perfusion<sup>32</sup> and ranges from 1 to 0. The homogeneity index, calculated as 1 minus the inhomogeneity index, is easier to understand, with higher values representing more homogeneous lung ventilation and perfusion.

### Statistical Analysis

A data analysis and statistical plan were written and filed with the study protocol approved by the local Institutional Ethical Committee before data were accessed. No sample size calculation was possible due to the lack of previous studies on the same main outcome. No imputation for missing data was applied, as all the analyzed cases were complete. Quantitative variables are expressed as median (interquartile range) and compared with the Wilcoxon–Mann–Whitney test. Categorical data are reported as absolute numbers and percentages and compared with the Fisher exact test. Changes between supine and prone positions are calculated and reported as medians and 95% CI. All statistical analyses were conducted with R version 4.0.5 (R Core Team, Austria).

### Results

We enrolled 30 consecutive patients after a median of 10 [interquartile range, 7 to 13] days since symptom onset and 4 [interquartile range, 2 to 7] days since hospital admission. The study enrollment flowchart is presented in figure 2, while patients' baseline characteristics are reported in table 1. Twenty-four patients (80%) were discharged alive from the ICU, after a median stay of 16 [interquartile range, 10 to 24] days. No electrical impedance tomography belt repositioning was necessary between measurements, after turning patients prone.

The variations after prone positioning, as compared to baseline values in the supine position, are shown in table 2.

The physiologic effects of 90 min of prone position varied among individuals, as indicated by different behavior in two sample patients, as depicted in figure 3. However, as shown in figure 4, there was an overall significant increase of ventilation–perfusion matching from 58% [interquartile range, 43 to 69%] to 68% [interquartile range, 56 to 75%] ( $P = 0.042$ ). Dead space area (40% [interquartile range, 27 to 55%] vs.

29% [interquartile range, 24 to 41%], for supine and prone position, respectively,  $P = 0.103$ ) and shunt area (2% [interquartile range, 1 to 4%] vs. 1% [interquartile range, 0 to 3%], for supine and prone position, respectively,  $P = 0.178$ ) did not vary between the two positions, while total mismatch area overall decreased from supine to prone (42% [interquartile range, 31 to 57%] vs. 32% [interquartile range, 25 to 43%], respectively,  $P = 0.045$ ). Prone positioning increased the proportion of dorsal lung ventilation from 39% [interquartile range, 31 to 43%] to 52% [interquartile range, 44 to 62%] ( $P < 0.001$ ; fig. 5A), while it did not affect dorsal perfusion (52% [interquartile range, 42 to 64%] vs. 57% [interquartile range, 50 to 61%],  $P = 0.224$ ; fig. 5B). Also shown in table 2, the median electrical impedance tomography–based optimal PEEP was no different between supine and prone position (14 [interquartile range, 12 to 15] cm H<sub>2</sub>O vs. 14 [interquartile range, 12 to 16] cm H<sub>2</sub>O, respectively,  $P = 0.086$ ). Individual data points are available as Supplemental Digital Content (<http://links.lww.com/ALN/C872>). Plateau pressure, driving pressure, and respiratory system quasi-static compliance did not show significant differences between supine and prone positions (fig. 6, A and B). The loss of lung compliance due to overdistension decreased with prone positioning from 9% [interquartile range, 4 to 11%] to 4% [interquartile range, 2 to 6%] ( $P = 0.025$ ; fig. 6C), while no variation was observed with respect to the loss of compliance secondary to lung collapse (4% [interquartile range, 2 to 7%] vs. 7% [interquartile range, 4 to 9%],  $P = 0.336$ ; fig. 6D).

Twenty-one patients (70%) were prone-responders.<sup>25</sup> The median PaO<sub>2</sub>/F<sub>IO</sub><sub>2</sub> increased from 141 [interquartile range, 104 to 182] mmHg to 235 [interquartile range, 164 to 267] mmHg ( $P < 0.001$ ), while Paco<sub>2</sub> and pH were no different between supine (45 [interquartile range, 40 to 52] mmHg and 7.38 [interquartile range, 7.31 to 7.43], respectively) and prone (45 [interquartile range, 42 to 52] mmHg and 7.37 [interquartile range, 7.33 to 7.42], respectively) position ( $P = 0.350$  and 0.611 for Paco<sub>2</sub> and pH, respectively). The oxygenation improvement allowed F<sub>IO</sub><sub>2</sub> reduction from 0.6 [interquartile range, 0.4 to 0.9] to 0.5 [interquartile range, 0.4 to 0.6] ( $P = 0.008$ ) after study protocol completion.

### Discussion

In this prospective observational study, conducted in intubated and mechanically ventilated COVID-19 ARDS patients, we found that (1) prone position was associated with increased ventilation–perfusion matching; (2) turning patients prone increased dorsal ventilation and reduced lung overdistension, while it did not affect dorsal perfusion, lung collapse, driving pressure, and respiratory system quasi-static compliance; and (3) after 90 min of prone position, PaO<sub>2</sub>/F<sub>IO</sub><sub>2</sub> overall increased, with 70% of patients classified as prone-responders.<sup>25</sup>

In a recent multicenter observational study evaluating the effects of prone positioning in 78 patients with COVID-19 ARDS, Langer *et al.* reported 78% of patients experiencing

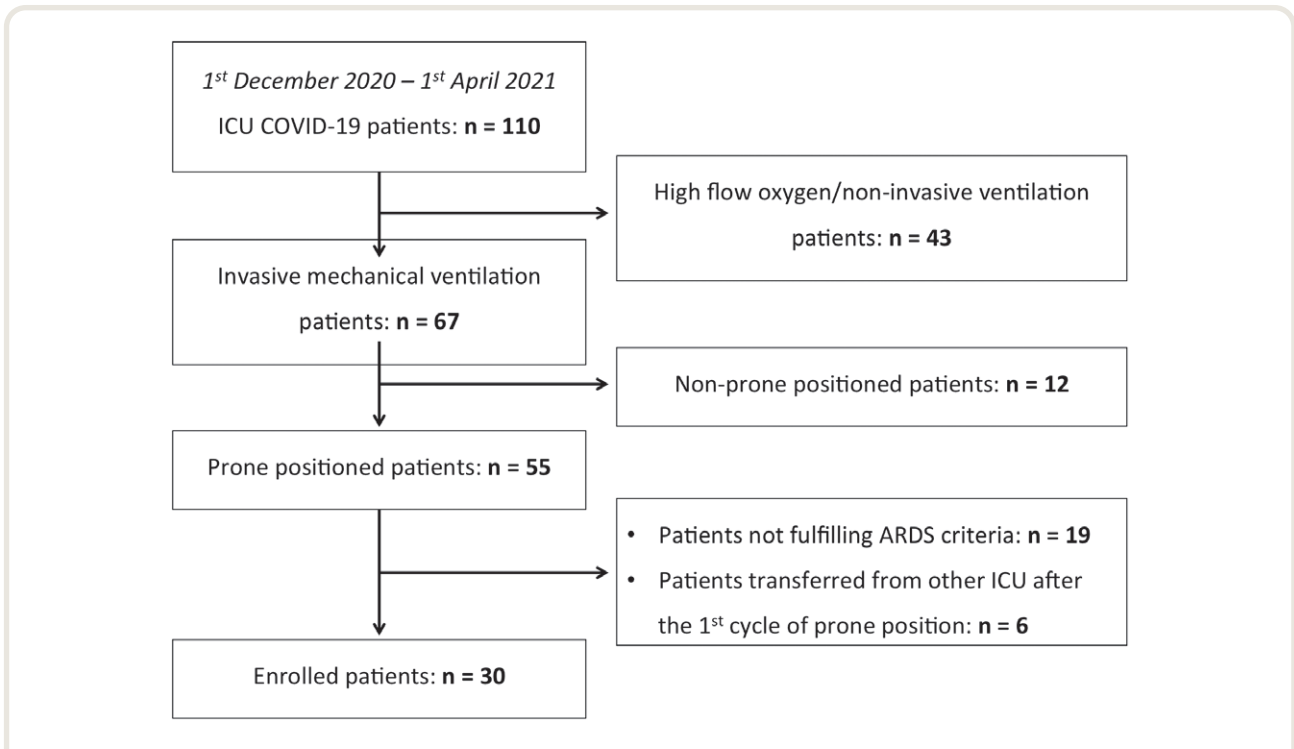


**Fig. 2.** Study enrollment flowchart. ARDS, acute respiratory distress syndrome; ICU, intensive care unit.

**Table 1.** Patients' Baseline Characteristics

Patients' Characteristics (n = 30)		Median [Interquartile Range] or n (%)
Demographic variables	Age (yr)	62 [53, 72]
	Weight (kg)	85 [77, 118]
	Body mass index (kg/m <sup>2</sup> )	29 [25, 38]
	Sex (male, n, %)	22 (73%)
	Arterial hypertension (n, %)	13 (43%)
	COPD (n, %)	2 (7%)
	SOFA score	4 [3, 4]
	Days since symptoms onset*	10 [7, 13]
	Days since hospital admission	4 [2, 7]
Laboratory and clinical data	Days since intubation	0 [0, 1]
	C-reactive protein (mg/l)	100 [55, 180]
	Procalcitonin (µg/l)	0.16 [0.07, 0.52]
	D-dimer (µg/l)	434 [210, 1090]
	Ferritin (µg/l)	670 [616, 1530]
Ventilator setting	Prone positioning cycle length (hours)	17.5 [14.2, 27.0]
	Tidal volume (ml/kg ideal body weight)	5.6 [5.6, 6.0]
	Respiratory rate (breaths/min)	22 [20, 22]

\*Symptoms compatible with severe acute respiratory syndrome COVID-2 infection were considered (cough, dyspnea, fever).  
COPD, chronic obstructive pulmonary disease; SOFA, Sequential Organ Failure Assessment.

an increase in Pao<sub>2</sub>/Fio<sub>2</sub> greater than or equal to 20 mmHg, without improving either driving pressure or respiratory system quasi-static compliance.<sup>14</sup> This finding led the authors to speculate that the main mechanism determining the improvement of arterial oxygenation during pronation of COVID-19 ARDS patients is not lung recruitment, but rather the

improvement of the ventilation-perfusion matching.<sup>14</sup> In keeping with the results of that study<sup>14</sup> and of another previous investigation,<sup>33</sup> we also found that prone positioning was not associated with improvement of respiratory system quasi-static compliance or driving pressure, which were recently correlated with ICU mortality in COVID-19 ARDS

**Table 2.** Variations between Supine and Prone Positions

		Supine	Prone	P Value	Difference (Median and 95% CI)
Ventilator setting	Fi <sub>o</sub> <sub>2</sub>	0.6 [0.4, 0.9]	0.5 [0.4, 0.6]	0.008‡	-0.20 (-0.07 to -0.37)
	PEEP (cm H <sub>2</sub> O)	14 [12, 15]	14 [12, 16]	0.086	1.0 (0.0 to 2.5)
Arterial blood gases	Pao <sub>2</sub> (mmHg)	80 [68, 92]	105 [85, 142]	< 0.001‡	30 (14 to 49)
	Pao <sub>2</sub> /Fio <sub>2</sub> (mmHg)	141 [104, 182]	235 [164, 267]	0.019‡	86.9 (118.8 to 57.7)
	Paco <sub>2</sub> (mmHg)	45 [40, 52]	45 [42, 52]	0.350	1.2 (-1.0 to 3.4)
	pH	7.38 [7.31, 7.43]	7.37 [7.33, 7.42]	0.611	0.00 (-0.02 to 0.01)
Respiratory mechanics	Plateau pressure (cm H <sub>2</sub> O)	23 [20, 26]	23 [22, 26]	0.335	0.50 (-0.99 to 1.99)
	Driving pressure (cm H <sub>2</sub> O)	11 [8, 11]	10 [9, 11]	0.656	0.0 (-1.0 to 0.5)
	Respiratory system quasi-static compliance (ml/cm H <sub>2</sub> O)	40 [34.5, 47.8]	39.1 [34.5, 50.0]	0.948	0.1 (-4.3 to 3.6)
Electrical impedance tomography-based variables	Dorsal ventilation (%)	39 [31, 43]	52 [44, 62]	< 0.001‡	16 (10 to 20)
	Dorsal perfusion (%)	52 [42, 64]	57 [50, 61]	0.224	3 (-3 to 10)
	Global homogeneity index ventilation	0.48 [0.47, 0.52]	0.50 [0.48, 0.54]	0.103	0.02 (0.00 to 0.04)
	Global homogeneity index perfusion	0.14 [0.05, 0.27]	0.25 [0.10, 0.33]	0.077	0.07 (0.00 to 0.15)
	Matched area (%)	58 [43, 69]	68 [56, 75]	0.042‡	8.0 (0.1 to 16.0)
	Dead space area (%)	40 [27, 55]	29 [24, 42]	0.103	-6.6 (-15.8 to 1.3)
	Shunt area (%)	2 [1, 4]	1 [0, 3]	0.178	-0.8 (-2.2 to 0.3)
	Total unmatched area (%)	42 [31, 57]	32 [25, 43]	0.045‡	-7.8 (-16.0 to -0.1)
	Dead space to shunt ratio	24 [7, 85]	18 [10, 78]	0.350	-6.6 (-55.3 to 28.5)
	Lung compliance loss as assessed by electrical impedance tomography lung overdistension (%)	9 [4, 11]	4 [2, 6]	0.025‡	-3.5 (-7.4 to -0.5)
	Lung compliance loss as assessed by electrical impedance tomography lung collapse (%)	4 [2, 7]	7 [4, 9]	0.336	1.2 (-1.5 to 4.0)
Hemodynamic variables*	Heart rate (beats per minute)	78 [67, 84]	75 [70, 87]	0.803	-1 (-4 to 3)
	MAP (mmHg)	62 [61, 64]	62 [61, 65]	0.802	-1 (-2 to 1)
	Hypotension requiring norepinephrine † (n, %)	23 (76.7)	22 (73.3)	1.000	

Data are expressed as median [interquartile range].

\*Hemodynamic variables were registered at the time of electrical impedance tomography perfusion assessment. †Norepinephrine was administered to assure a mean arterial pressure greater than 60 mmHg, with doses ranging from 0.05 to 0.2mcg/kg·min. ‡P values less than 0.05

Fi<sub>o</sub><sub>2</sub>, fractional inspired oxygen tension; MAP, mean arterial pressure; PEEP, positive end-expiratory pressure.

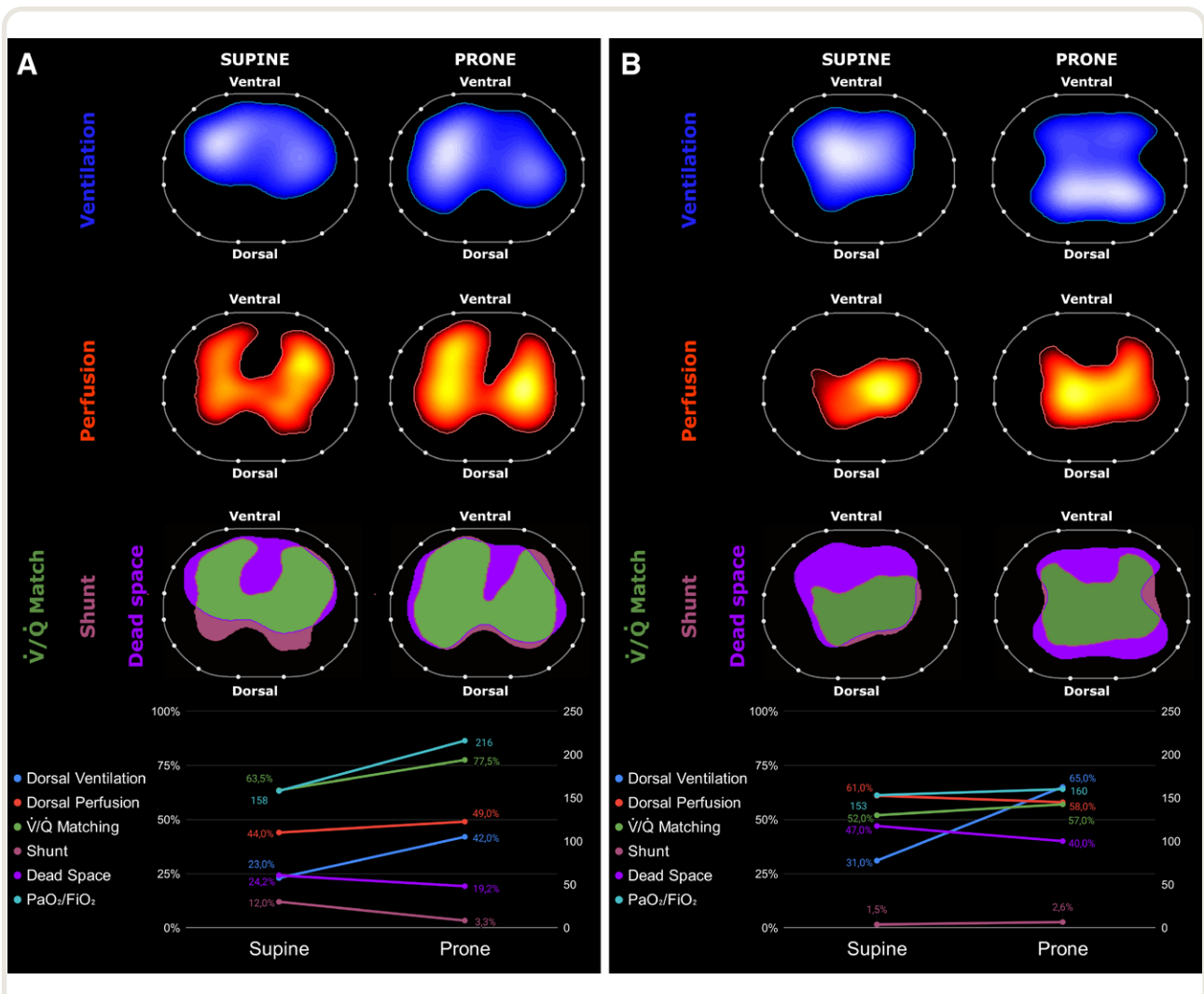
patients.<sup>34</sup> Nonetheless, since we did not separately measure lung and chest wall compliance, the latter known to decrease in prone position,<sup>15</sup> we cannot exclude that lung compliance actually improved, as also suggested by the increased dorsal ventilation and the reduced lung overdistension. Worth remarking, in agreement with Perier *et al.*,<sup>35</sup> electrical impedance tomography-based optimal PEEP value, as defined by the best compromise between lung overdistension and collapse, was no different between the supine and prone positions, further confirming the hypothesis by Langer *et al.*<sup>14</sup>

In keeping with Perier *et al.*, who assessed electrical impedance tomography perfusion in nine patients with COVID-19 ARDS,<sup>36</sup> we found that prone positioning did not alter the distribution of lung perfusion, which remained predominantly in the dorsal areas. However, different from Perier *et al.*,<sup>36</sup> who did not evaluate the total mismatch, we observed an increased ventilation-perfusion matching. Unlike Perier *et al.*,<sup>36</sup> who measured cardiac output to assess ventilation to perfusion ratio and reported a reduction in dead space, primarily consequent to changes in ventilation distribution in the ventral area, without a decrease in shunt, we did not find significant variations in both shunt and dead space between the supine and prone positions. Differences in the technique adopted and in the timing of assessment, and, worth remarking, a definitely larger sample size, may

all contribute to explaining these discrepancies. Indeed, the baseline dead space values found in the current study are in keeping with those reported in a previous case series assessing shunt and dead space through electrical impedance tomography in the supine position.<sup>12</sup> Different from that study,<sup>12</sup> however, we found very low values of baseline shunt, likely ascribable to the fact that we included patients at an early stage of disease, when low ventilation-perfusion ratio due to the loss of regulation of perfusion and hypoxic vasoconstriction may be the main factor in determining hypoxemia, as already proposed by Gattinoni *et al.*<sup>37</sup>

In keeping with our previous observation describing the increased ventilation-perfusion matching after prone positioning in a single COVID-19 ARDS patient,<sup>17</sup> and supporting the hypothesis deriving from previous investigations,<sup>14</sup> the current study shows that an improvement in ventilation-perfusion matching rather than lung recruitment is the main mechanism for oxygenation amelioration in the prone position. It is important to remark, however, that the extent of ventilation-perfusion matching amelioration was just 10%, which might explain why we did not observe a concomitant reduction of Paco<sub>2</sub>, whose median baseline value, worth remarking, was not altered.

Despite the overall increase in ventilation-perfusion matching, our population shows a heterogeneous response



Downloaded from <http://asa2.silverchair.com/anesthesiology/article-pdf/137/3/327/692802/20220900-0-00014.pdf> by guest on 19 April 2024

**Fig. 3.** Effects of prone positioning on ventilation and perfusion, as evaluated by electrical impedance tomography, in two representative patients. From top to bottom, lung ventilation (blue-white gradient area), perfusion (red-yellow area), and ventilation-perfusion ( $\dot{V}/\dot{Q}$ ) matching are depicted. The graph at the bottom provides variations of dorsal ventilation and perfusion,  $\dot{V}/\dot{Q}$  matching, shunt, dead space, and  $\text{PaO}_2/\text{FiO}_2$  values in the supine and prone positions. The first patient (A) exhibits improved  $\text{PaO}_2/\text{FiO}_2$  and increased distribution of ventilation to the dorsal regions, resulting in improvement of  $\dot{V}/\dot{Q}$  matching. The second patient (B) does not improve  $\text{PaO}_2/\text{FiO}_2$  and shows no increase in  $\dot{V}/\dot{Q}$  matching despite increased dorsal ventilation.  $\text{FiO}_2$ , fractional inspired oxygen tension.

to pronation among patients, as shown in figures 3, 4, and 5, thus suggesting other potential mechanisms underlining the improvement in oxygenation secondary to prone positioning. Although the COVID-19 pandemic led some authors to question the definition of ARDS itself,<sup>38,39</sup> similar to “typical” ARDS,<sup>4</sup> COVID-19 ARDS is *per se* a heterogeneous disorder combining various pathologic features (tracheobronchitis, diffuse alveolar damage, and vascular injury).<sup>7</sup> If on the one hand the pulmonary vessels are characterized by inflammation, vasculitis, microthrombi, and, in some cases, macrothrombi, on the other hand, viral infection in areas of ongoing active injury contributes to persistent and temporally heterogeneous lung damage.<sup>7</sup> Virus-related pathophysiologic injuries affect to varying extents both alveoli and pulmonary vasculature, resulting in

different pathologic phenotypes.<sup>8</sup> Such heterogeneity cautions ICU physicians on basing COVID-19 treatments on simplistic phenotypic models and highlights the role of a more comprehensive and individualized ventilatory management.

A point of strength of our study is that our patient population is quite homogenous, as it includes patients (1) with moderate ARDS due to the same etiology, (2) at the first cycle of prone positioning, (3) in the first day after endotracheal intubation (thus justifying the moderate severity of the disease), and (4) enrolled after a maximum of 11 days since hospital admission, thereby limiting (a) the risk of confounding factors, such as ventilator-associated pneumonia, and (b) the potential loss of prone responsiveness observed in the advanced phases of the disease.<sup>40</sup>

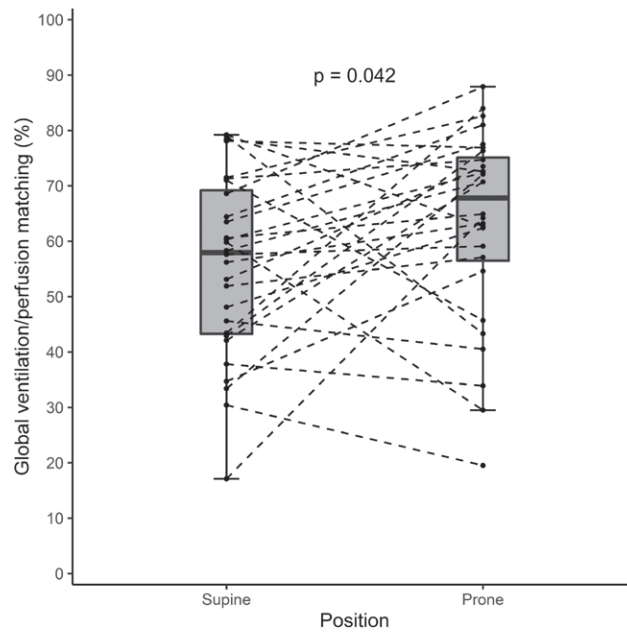


**Fig. 4.** Percentage of ventilation-perfusion matching, as assessed by electrical impedance tomography, in the supine and prone position. The *boxplot's* hinges represent the first and third quartile of the data, the *upper and lower whiskers* indicate the highest and lowest values within 1.5 times the interquartile range, and the *bold line* indicates the median. Individual data points are also plotted, with *dashed lines* connecting the two measurements in the supine and prone position.

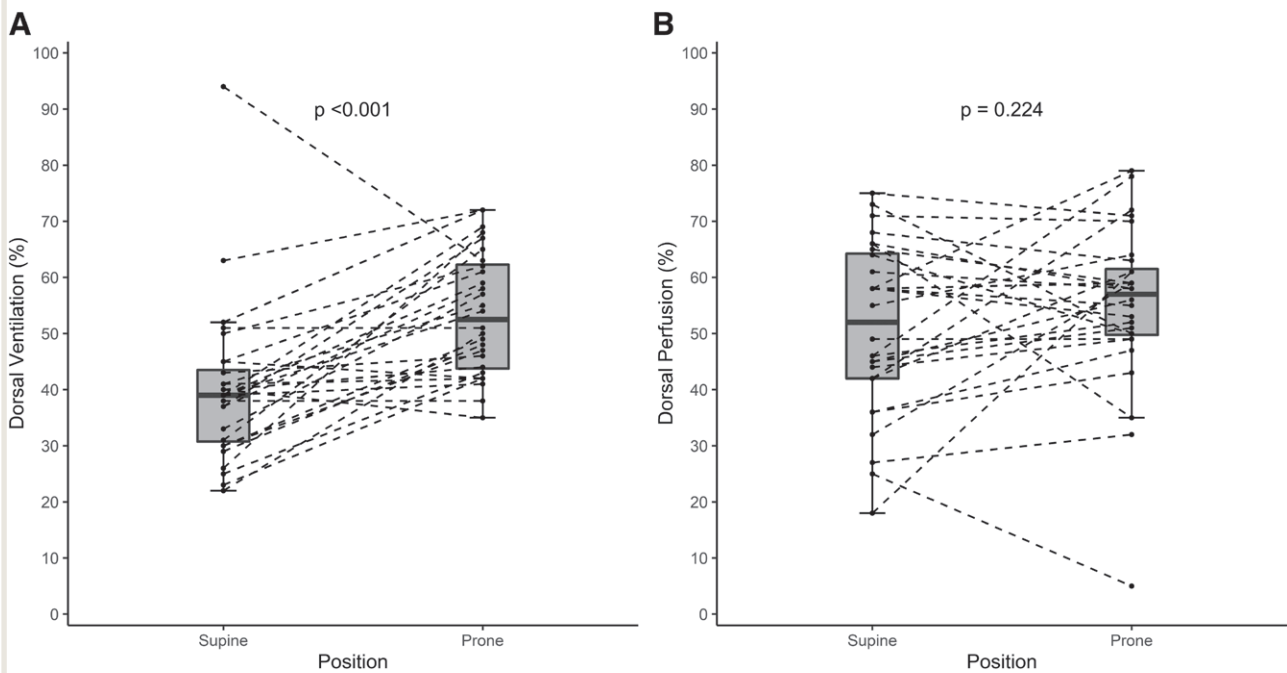
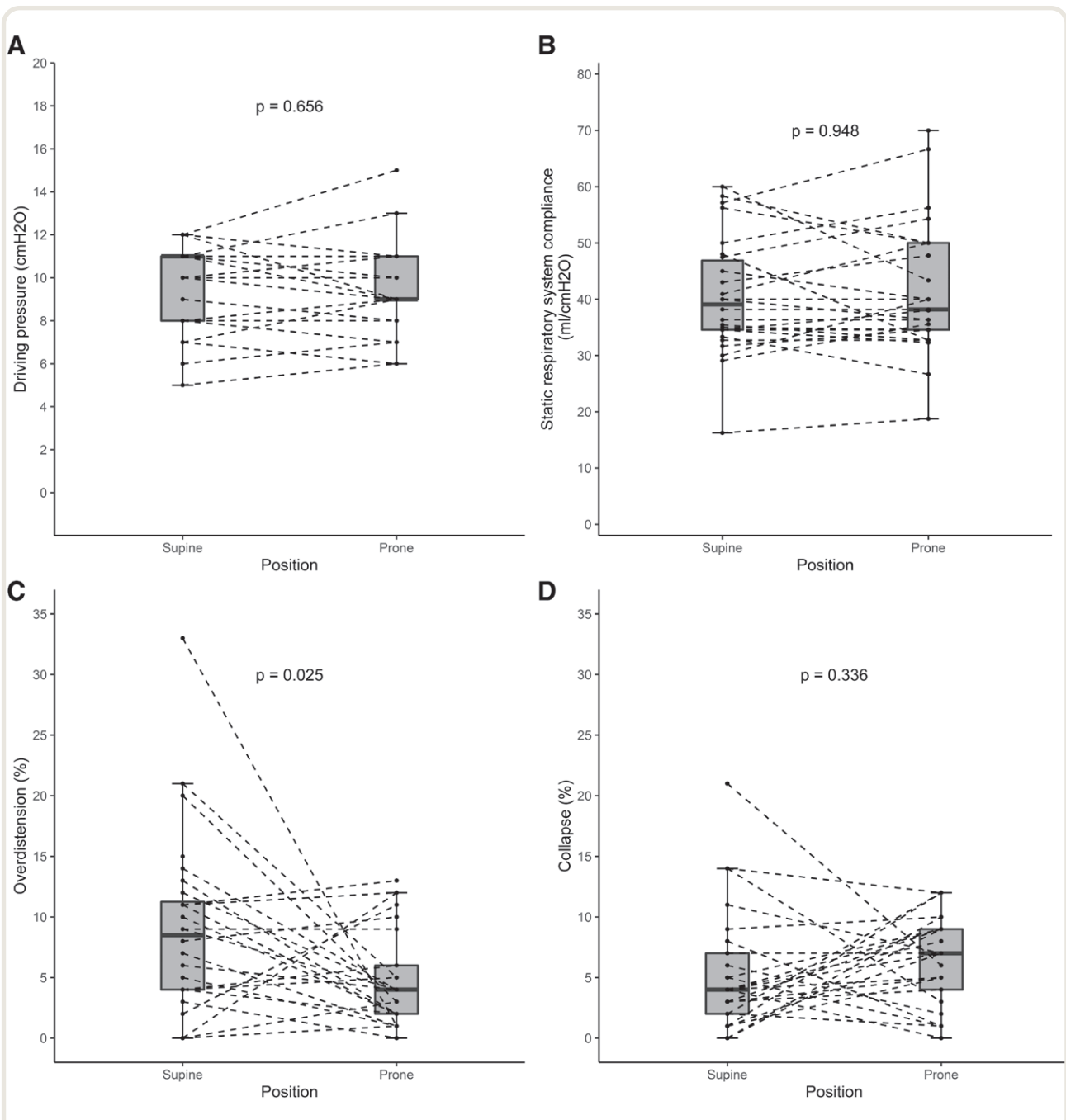


**Fig. 5.** Percentage of ventilation (A) and perfusion (B) of the dorsal part of the lung, as assessed by electrical impedance tomography, in the supine and prone positions. The *boxplot's* hinges represent the first and third quartile of the data, the *upper and lower whiskers* indicate the highest and lowest values within 1.5 times the interquartile range, and the *bold line* indicates the median. Individual data points are also plotted, with *dashed lines* connecting the two measurements in the supine and prone position.





Downloaded from <http://esa2.silverchair.com/anesthesiology/article-pdf/137/3/327/692802/20220900.0-00014.pdf> by guest on 19 April 2024

**Fig. 6.** Driving pressure (A) and static compliance of the respiratory system (B) before and after prone positioning. Percentage of lung compliance loss due to overdistension (C) and collapse (D) as assessed by electrical impedance tomography before and after prone positioning. Positive end-expiratory pressure was selected as the best compromise between overdistension and collapse at both time points. The *boxplots*'s hinges represent the first and third quartile of the data, the *upper and lower whiskers* indicate the highest and lowest values within 1.5 times the interquartile range, and the *bold line* indicates the median. Individual data points are also plotted, with *dashed lines* connecting the two measurements in the supine and prone positions.

Our study has several limitations. No causal inferences can reliably be drawn due to the pre–post design in a single group without controls, since several measured and unmeasured factors may interfere during the study period. Moreover, although we explored a much larger patient population than

in previous similar physiologic investigations,<sup>12,36</sup> we cannot exclude that our study was not adequately powered.

It is important that electrical impedance tomography perfusion assessment by slope analysis of saline dilution is still experimental and has been validated only in two animal studies.<sup>31,41</sup>

In particular, Bluth *et al.*<sup>31</sup> conducted a head-to-head comparison between a reference standard technique (positron emission tomography) and electrical impedance tomography in pigs. The authors found that electrical impedance tomography underestimated the relative perfusion in the dependent thoracic regions, and overestimated it in the nondependent ones, partly ascribable to software limitations, related to anatomical characteristics of the animals, and incomplete masking of the heart region. This possibly incorrect estimation of perfusion in dependent/nondependent regions might lead to a decreased ventral-dorsal gradient of lung perfusion and then to a reduced estimation of ventilation-perfusion matching. Worth mentioning, however, compared to the work of Bluth *et al.*,<sup>31</sup> we used a more advanced version of the electrical impedance tomography perfusion software. Also, electrical impedance tomography has a limited spatial resolution and explores only the area of the lung surrounded by the belt, which might not be representative of the whole pulmonary parenchyma.<sup>24</sup>

In keeping with a previous study,<sup>36</sup> we assessed the early effects of prone position to guarantee a stable position of the electrical impedance tomography belt between measurements, which is of paramount importance considering our study design.<sup>24</sup> Nevertheless, since prone positioning is commonly applied for much longer periods of time, we cannot exclude that the number of responders was underestimated, as some patients might have shown a later response. Moreover, as in previous studies exploring the response to prone positioning,<sup>14,25</sup> we did not assess the oxygenation response when the patient was turned back to the supine position.

Finally, we neither measured esophageal pressure to partition the chest wall and lung compliances nor systematically ruled out pulmonary thromboembolism in all our patients. It is worth mentioning that all patients were treated with intermediate doses of low-molecular-weight heparin,<sup>24</sup> and in nine patients (30%) who underwent computed tomography pulmonary angiography for clinical indications, we found no thromboembolic involvement of major lung vessels.

## Conclusions

In this observational study in COVID-19 ARDS patients undergoing invasive mechanical ventilation, early prone positioning was overall associated with improved ventilation-perfusion matching, increased dorsal ventilation, reduced overdistension, and increased  $\text{PaO}_2/\text{FiO}_2$ , while not affecting dorsal perfusion, lung collapse, driving pressure, and respiratory system quasi-static compliance. These physiologic effects were, nonetheless, heterogeneous among patients.

Further larger clinical studies are necessary to assess whether the electrical impedance tomography analysis could reliably predict prone responsiveness based on early variations in the distribution of lung ventilation and perfusion.

## Acknowledgments

The authors thank all Institute of Anesthesia and Resuscitation 3 ICU personnel who made this work possible. In particular,

the authors are indebted to Michele Salvagno, M.D., Matteo Perona, M.D., Michele Della Paolera, M.D., Paolo Persona, M.D., Luisa Muraro, M.D., Arianna Peralta, M.D., Enrico Petranzan, M.D., and Eugenio Serra, M.D., all from the Institute of Anesthesia and Intensive Care, Padua University Hospital, Padua, Italy, for their invaluable help in data collection. Last but not least, the authors must acknowledge Dario Gregori, Ph.D. (Unit of Biostatistics, Epidemiology, and Public Health, Department of Cardiac, Thoracic, and Vascular Sciences, University of Padova, Padova, Italy) for his statistical advice. Availability of supporting data: The data that support the findings of this study are available from the corresponding author, Dr. Navalesi, upon request.

## Research Support

This research did not receive any specific grant from funding agencies in the public, commercial, or not-for-profit sectors. The software for electrical impedance tomography perfusion analysis was kindly provided by Draeger (Lubeck, Germany) for research purposes.

## Competing Interests

Dr. Navalesi receives royalties from Intersurgical SPA (Mirandola, Italy) for the Helmet Next invention. He also received speaking fees from Draeger (Lubeck, Germany), Intersurgical SPA, Getinge (Goteborg, Sweden), MSD (Rahway, New Jersey), Gilead (Foster City, California), Philips (Milan, Italy), Respmid (El Paso, Texas), and Novartis (Basel, Switzerland). His research laboratory received research grants and/or research equipment from Intersurgical SPA, Draeger, and Gilead. The other authors declare no competing interests.

## Correspondence

Address correspondence to Dr. Navalesi: via V. Gallucci 13, 35125 Padova, Italy. paolo.navalesi@unipd.it. This article may be accessed for personal use at no charge through the Journal Web site, [www.anesthesiology.org](http://www.anesthesiology.org).

## Supplemental Digital Content

Strengthening the Reporting of Observational Studies in Epidemiology Checklist and Supplemental Figure, <http://links.lww.com/ALN/C872>

## References

- Grieco DL, Bongiovanni F, Chen L, Menga LS, Cutuli SL, Pintaudi G, Carelli S, Michi T, Torrini F, Lombardi G, Anzellotti GM, De Pascale G, Urbani A, Bocci MG, Tanzarella ES, Bello G, Dell'Anna AM, Maggiore SM, Brochard L, Antonelli M: Respiratory physiology of COVID-19-induced respiratory failure compared to ARDS of other etiologies. *Crit Care* 2020; 24:529

2. Fan E, Beitler JR, Brochard L, Calfee CS, Ferguson ND, Slutsky AS, Brodie D: COVID-19-associated acute respiratory distress syndrome: Is a different approach to management warranted? *Lancet Respir Med* 2020; 8:816–21
3. Grasselli G, Tonetti T, Protti A, Langer T, Girardis M, Bellani G, Laffey J, Carrafiello G, Carsana L, Rizzuto C, Zanella A, Scaravilli V, Pizzilli G, Grieco DL, Di Meglio L, de Pascale G, Lanza E, Monteduro F, Zompatori M, Filippini C, Locatelli F, Cecconi M, Fumagalli R, Nava S, Vincent JL, Antonelli M, Slutsky AS, Pesenti A, Ranieri VM; collaborators: Pathophysiology of COVID-19-associated acute respiratory distress syndrome: A multicentre prospective observational study. *Lancet Respir Med* 2020; 8:1201–8
4. Grasselli G, Cattaneo E, Florio G, Ippolito M, Zanella A, Cortegiani A, Huang J, Pesenti A, Einav S: Mechanical ventilation parameters in critically ill COVID-19 patients: A scoping review. *Crit Care* 2021; 25:115
5. Tonetti T, Grasselli G, Rucci P, Alessandri F, Dell'Olio A, Boscolo A, Pasin L, Sella N, Mega C, Melotti RM, Girardis M, Busani S, Bellani G, Foti G, Grieco DL, Scaravilli V, Protti A, Langer T, Mascia L, Pugliese F, Cecconi M, Fumagalli R, Nava S, Antonelli M, Slutsky AS, Navalesi P, Pesenti A, Ranieri VM: Synergistic effect of static compliance and D-dimers to predict outcome of patients with COVID-19-ARDS: A prospective multicenter study. *Biomedicine* 2021; 9:1228
6. Chiumello D, Busana M, Coppola S, Romitti F, Formenti P, Bonifazi M, Pozzi T, Palumbo MM, Cressoni M, Herrmann P, Meissner K, Quintel M, Camporota L, Marini JJ, Gattinoni L: Physiological and quantitative CT-scan characterization of COVID-19 and typical ARDS: A matched cohort study. *Intensive Care Med* 2020; 46:2187–96
7. Borczuk AC, Salvatore SP, Seshan SV, Patel SS, Bussell JB, Mostyka M, Elsoukary S, He B, Del Vecchio C, Fortarezza F, Pezzuto F, Navalesi P, Crisanti A, Fowkes ME, Bryce CH, Calabrese F, Beasley MB: COVID-19 pulmonary pathology: A multi-institutional autopsy cohort from Italy and New York City. *Mod Pathol* 2020; 33:2156–68
8. Calabrese F, Pezzuto F, Fortarezza F, Boscolo A, Lunardi F, Giraudo C, Cattelan A, Del Vecchio C, Lorenzoni G, Vedovelli L, Sella N, Rossato M, Rea F, Vettor R, Plebani M, Cozzi E, Crisanti A, Navalesi P, Gregori D: Machine learning-based analysis of alveolar and vascular injury in SARS-CoV-2 acute respiratory failure. *J Pathol* 2021; 254:173–84
9. Boscolo A, Spiezia L, Correale C, Sella N, Pesenti E, Beghetto L, Campello E, Poletto F, Cerruti L, Cola M, De Cassai A, Pasin L, Eugenio S, Vettor R, Cattelan AM, Simioni P, Navalesi P: Different hypercoagulable profiles in patients with COVID-19 admitted to the internal medicine ward and the intensive care unit. *Thromb Haemost* 2020; 120:1474–7
10. Santamarina MG, Boisier D, Contreras R, Baque M, Volpacchio M, Beddings I: COVID-19: A hypothesis regarding the ventilation-perfusion mismatch. *Crit Care* 2020; 24:395
11. Santamarina MG, Boisier Riscal D, Beddings I, Contreras R, Baque M, Volpacchio M, Martinez Lomakin F: COVID-19: What iodine maps from perfusion CT can reveal—A prospective cohort study. *Crit Care* 2020; 24:619
12. Mauri T, Spinelli E, Scotti E, Colussi G, Basile MC, Crotti S, Tubiolo D, Tagliabue P, Zanella A, Grasselli G, Pesenti A: Potential for lung recruitment and ventilation-perfusion mismatch in patients with the acute respiratory distress syndrome from coronavirus disease 2019. *Crit Care Med* 2020; 48:1129–34
13. Spinelli E, Kircher M, Stender B, Ottaviani I, Basile MC, Marongiu I, Colussi G, Grasselli G, Pesenti A, Mauri T: Unmatched ventilation and perfusion measured by electrical impedance tomography predicts the outcome of ARDS. *Crit Care* 2021; 25:192
14. Langer T, Brioni M, Guzzardella A, Carlesso E, Cabrini L, Castelli G, Dalla Corte F, De Robertis E, Favaro M, Forastieri A, Forlini C, Girardis M, Grieco DL, Mirabella L, Noseda V, Previtali P, Protti A, Rona R, Tardini F, Tonetti T, Zannoni F, Antonelli M, Foti G, Ranieri M, Pesenti A, Fumagalli R, Grasselli G; PRONA-COVID Group: Prone position in intubated, mechanically ventilated patients with COVID-19: A multi-centric study of more than 1000 patients. *Crit Care* 2021; 25:128
15. Guérin C, Albert RK, Beitler J, Gattinoni L, Jaber S, Marini JJ, Munshi L, Papazian L, Pesenti A, Vieillard-Baron A, Mancebo J: Prone position in ARDS patients: Why, when, how and for whom. *Intensive Care Med* 2020; 46:2385–96
16. Dalla Corte F, Mauri T, Spinelli E, Lazzeri M, Turrini C, Albanese M, Abbruzzese C, Lissoni A, Galazzi A, Eronia N, Bronco A, Maffezzini E, Pesenti A, Foti G, Bellani G, Grasselli G: Dynamic bedside assessment of the physiologic effects of prone position in acute respiratory distress syndrome patients by electrical impedance tomography. *Minerva Anestesiologia* 2020; 86:1057–64
17. Zarantonello F, Andreatta G, Sella N, Navalesi P: Prone position and lung ventilation and perfusion matching in acute respiratory failure due to COVID-19. *Am J Respir Crit Care Med* 2020; 202:278–9
18. von Elm E, Altman DG, Egger M, Pocock SJ, Gøtzsche PC, Vandenbroucke JP; STROBE Initiative: The Strengthening the Reporting of Observational Studies in Epidemiology (STROBE) statement: Guidelines for reporting observational studies. *J Clin Epidemiol* 2008; 61:344–9

19. Ranieri VM, Rubenfeld GD, Thompson BT, Ferguson ND, Caldwell E, Fan E, Camporota L, Slutsky AS; ARDS Definition Task Force: Acute respiratory distress syndrome: The Berlin Definition. *JAMA* 2012; 307:2526–33
20. World Health Organization. (2020) Clinical management of COVID-19: interim guidance, 27 May 2020. World Health Organization. Available at <https://apps.who.int/iris/handle/10665/332196>. Accessed July 7, 2022.
21. Pasin L, Sella N, Correale C, Boscolo A, Rosi P, Saia M, Mantoan D, Navalesi P: Regional COVID-19 network for coordination of SARS-CoV-2 outbreak in Veneto, Italy. *J Cardiothorac Vasc Anesth* 2020; 34:2341–5
22. Pasin L, Navalesi P, Zangrillo A, Kuzovlev A, Likhvantsev V, Hajjar LA, Fresilli S, Lacerda MVG, Landoni G: Corticosteroids for patients with coronavirus disease 2019 (COVID-19) with different disease severity: A meta-analysis of randomized clinical trials. *J Cardiothorac Vasc Anesth* 2021; 35:578–84
23. Meizlish ML, Goshua G, Liu Y, Fine R, Amin K, Chang E, DeFilippo N, Keating C, Liu Y, Mankbadi M, McManus D, Wang SY, Price C, Bona RD, Ochoa Chara CI, Chun HJ, Pine AB, Rinder HM, Siner JM, Neuberger DS, Owusu KA, Lee AI: Intermediate-dose anticoagulation, aspirin, and in-hospital mortality in COVID-19: A propensity score-matched analysis. *Am J Hematol* 2021; 96:471–9
24. Sella N, Pettenuzzo T, Zarantonello F, Andreatta G, De Cassai A, Schiavolin C, Simoni C, Pasin L, Boscolo A, Navalesi P: Electrical impedance tomography: A compass for the safe route to optimal PEEP. *Respir Med* 2021; 187:106555
25. Nakos G, Tsangaris I, Kostanti E, Nathanail C, Lachana A, Koulouras V, Kastani D: Effect of the prone position on patients with hydrostatic pulmonary edema compared with patients with acute respiratory distress syndrome and pulmonary fibrosis. *Am J Respir Crit Care Med* 2000; 161(2 pt 1):360–8
26. Bellani G, Laffey JG, Pham T, Fan E, Brochard L, Esteban A, Gattinoni L, van Haren F, Larsson A, McAuley DF, Ranieri M, Rubenfeld G, Thompson BT, Wrigge H, Slutsky AS, Pesenti A; LUNG SAFE Investigators; ESICM Trials Group: Epidemiology, patterns of care, and mortality for patients with acute respiratory distress syndrome in intensive care units in 50 countries. *JAMA* 2016; 315:788–800
27. Sella N, Zarantonello F, Andreatta G, Gagliardi V, Boscolo A, Navalesi P: Positive end-expiratory pressure titration in COVID-19 acute respiratory failure: Electrical impedance tomography vs. PEEP/FiO2 tables. *Crit Care* 2020; 24:540
28. Brower RG, Lancken PN, MacIntyre N, Matthay MA, Morris A, Ancukiewicz M, Schoenfeld D, Thompson BT; National Heart, Lung, and Blood Institute ARDS Clinical Trials Network: Higher *versus* lower positive end-expiratory pressures in patients with the acute respiratory distress syndrome. *N Engl J Med* 2004; 351:327–36
29. Amato MB, Meade MO, Slutsky AS, Brochard L, Costa EL, Schoenfeld DA, Stewart TE, Briel M, Talmor D, Mercat A, Richard JC, Carvalho CR, Brower RG: Driving pressure and survival in the acute respiratory distress syndrome. *N Engl J Med* 2015; 372:747–55
30. Zarantonello F, Sella N, Pettenuzzo T, Andreatta G, Dell'Amore A, Giraudo C, Rea F, Navalesi P: Bedside detection and follow-up of pulmonary artery stenosis after lung transplantation. *Am J Respir Crit Care Med* 2021; 204:1100–2
31. Bluth T, Kiss T, Kircher M, Braune A, Bozsak C, Huhle R, Scharffenberg M, Herzog M, Roegner J, Herzog P, Vivona L, Millone M, Dössel O, Andreeff M, Koch T, Kotzerke J, Stender B, Gama de Abreu M: Measurement of relative lung perfusion with electrical impedance and positron emission tomography: An experimental comparative study in pigs. *Br J Anaesth* 2019; 123:246–54
32. Zhao Z, Möller K, Steinmann D, Frerichs I, Guttman J: Evaluation of an electrical impedance tomography-based Global Inhomogeneity Index for pulmonary ventilation distribution. *Intensive Care Med* 2009; 35:1900–6
33. Carsetti A, Damia Paciarini A, Marini B, Pantanetti S, Adrario E, Donati A: Prolonged prone position ventilation for SARS-CoV-2 patients is feasible and effective. *Crit Care* 2020; 24:225
34. Boscolo A, Sella N, Lorenzoni G, Pettenuzzo T, Pasin L, Pretto C, Tocco M, Tamburini E, De Cassai A, Rosi P, Polati E, Donadello K, Gottin L, De Rosa S, Baratto F, Toffoletto F, Ranieri VM, Gregori D, Navalesi P; COVID-19 VENETO ICU Network: Static compliance and driving pressure are associated with ICU mortality in intubated COVID-19 ARDS. *Crit Care* 2021; 25:263
35. Perier F, Tuffet S, Maraffi T, Alcalá G, Victor M, Haudebourg AF, Razazi K, De Prost N, Amato M, Carteaux G, Mekontso Dessap A: Electrical impedance tomography to titrate positive end-expiratory pressure in COVID-19 acute respiratory distress syndrome. *Crit Care* 2020; 24:678
36. Perier F, Tuffet S, Maraffi T, Alcalá G, Victor M, Haudebourg AF, De Prost N, Amato M, Carteaux G, Mekontso Dessap A: Effect of positive end-expiratory pressure and proning on ventilation and perfusion in COVID-19 acute respiratory distress syndrome. *Am J Respir Crit Care Med* 2020; 202:1713–7
37. Gattinoni L, Chiumello D, Caironi P, Busana M, Romitti F, Brazzi L, Camporota L: COVID-19 pneumonia: Different respiratory treatments for

- different phenotypes? *Intensive Care Med* 2020; 46:1099–102
38. Gattinoni L, Marini JJ: Isn't it time to abandon ARDS? The COVID-19 lesson. *Crit Care* 2021; 25:326
  39. Tobin MJ: Does making a diagnosis of ARDS in patients with coronavirus disease 2019 matter? *Chest* 2020; 158:2275–7
  40. Patel BV, Haar S, Handslip R, Auepanwiriyaikul C, Lee TM, Patel S, Harston JA, Hosking-Jervis F, Kelly D, Sanderson B, Borgatta B, Tatham K, Welters I, Camporota L, Gordon AC, Komorowski M, Antcliffe D, Prowle JR, Puthuchery Z, Faisal AA; United Kingdom COVID-ICU National Service Evaluation: Natural history, trajectory, and management of mechanically ventilated COVID-19 patients in the United Kingdom. *Intensive Care Med* 2021; 47:549–65
  41. Borges JB, Suarez-Sipmann F, Bohm SH, Tusman G, Melo A, Maripuu E, Sandström M, Park M, Costa EL, Hedenstierna G, Amato M: Regional lung perfusion estimated by electrical impedance tomography in a piglet model of lung collapse. *J Appl Physiol* (1985) 2012; 112:225–36

## ANESTHESIOLOGY REFLECTIONS FROM THE WOOD LIBRARY-MUSEUM

### Sertürner Isolates Morphine! And Eventually...Himself



Orphaned at age 15, Friedrich Wilhelm Sertürner (1783 to 1841, *right*) soon became a pharmacy apprentice at the court in Paderborn, Prussia. During his free time, he researched opium (*lower left*), the wondrous latex that oozed from scored poppy bulbs (*upper left*). While experimenting with a myriad of solvents in 1804, Sertürner discovered that ammonia applied to opium led to the formation of “completely colorless and regular” crystals. He named this pure alkali “morphium,” after Morpheus, the Greek god of dreams. When morphium relieved a toothache that opium could barely touch, Sertürner convinced three teenagers to help him explore its physical effects. After consuming a total of 90mg each, the four young men fell ill with “stomachache, weakness, and marked stupefaction bordering on unconsciousness.” Subsequent ingestion of vinegar provoked retching; constipation, stupor, and headache lingered for days. Sertürner reported his findings in an 1817 paper that captivated French chemist Joseph Louis Gay-Lussac, who renamed the substance “morphine” with the suffix “-ine” to herald the birth of the alkaloid class. With opium’s active ingredient now isolated, analgesia could be dosed incrementally. But while morphine decreased the risk of overdose from variably potent opium, it could still engender addiction. Sertürner himself became hooked on the drug and grew increasingly isolated with time. (Copyright © the American Society of Anesthesiologists’ Wood Library-Museum of Anesthesiology. [www.woodlibrarymuseum.org](http://www.woodlibrarymuseum.org))

Jane S. Moon, M.D., Assistant Clinical Professor, Department of Anesthesiology and Perioperative Medicine, University of California, Los Angeles, California.